

# Assessing the Impacts of Future 2°C Global Warming on Southern Ocean Cetaceans

CYNTHIA TYNAN

Associated Scientists at Woods Hole, Woods Hole, MA, USA

JOELLEN RUSSELL

Department of Geosciences, University of Arizona, Tucson, AZ, USA

## Abstract

Predicting the impact of global warming on polar marine ecosystems requires the combined efforts of climate modelers and marine ecologists. A subset of Intergovernmental Panel on Climate Change (IPCC) Fourth Assessment Report (AR4) climate model output for emission scenario ‘Special Report on Emission Scenarios’ (SRES) A1B (doubling of CO<sub>2</sub> from 360 and stabilizing at 720 after 2100) was used to identify the time period at which globally-averaged surface air temperature will have increased by 2°C above pre-industrial levels. Criteria used to identify a subset of the better IPCC AR4 climate-model outputs for emissions-scenario A1B are provided, and an *ensemble* of models is selected to examine impacts on cetaceans in the Southern Ocean. The potential impacts of the predicted change in Southern Ocean sea-ice extent, concentration and seasonality, water masses, ocean circulation and frontal positions on resident cetacean populations (i.e. Antarctic minke whales *Balaenoptera bonaerensis*) and migratory cetaceans are examined for the time of 2°C warming. Varying with specific Southern Ocean sector, Antarctic minke whales are expected to lose 5-30% of ice-associated habitat in the Antarctic by the year of 2°C warming (i.e., 2042 for the ensemble average). Migratory cetaceans will travel farther (~3-5° latitude) to reach important Southern Ocean fronts where they forage. The potential impact of the southward displacement of Southern Ocean fronts and watermass boundaries (i.e. Polar Front and Southern Boundary of the ACC) is a reduction and compression of the frontal-associated habitat of Southern Ocean cetaceans around Antarctica. As these frontal features are seasonally important to migratory cetaceans (i.e., blue whale *Balaenoptera musculus*, humpback whale *Megaptera novaeangliae*, fin whale *Balaenoptera physalus*, and sperm whale *Physeter macrocephalus*), it suggests a compression and reduction of valuable foraging habitat. The loss of 5-30% of ice cover is expected to reduce the availability of krill *Euphausia superba* upon which resident and migratory cetaceans, and the Antarctic ecosystem, depends.

## Introduction

In order to make predictions about the future of cetacean populations in the Southern Ocean, it is necessary to predict how their physical environment – namely water mass and frontal locations, ice conditions, air temperatures, winds, and sea surface temperatures – will change. Unfortunately, the climate models considered as part of the Intergovernmental Panel on Climate Change (IPCC) Fourth Assessment Report (AR4) produce conflicting estimates of changes in the Southern Ocean, largely because the models differ substantially in their ability to simulate the strength and position of the Southern Hemisphere westerly winds as well as other processes associated with the ocean component of the climate models (Russell et al., 2006). A poor simulation of the Southern Hemisphere atmospheric jet greatly distorts the oceanic simulation because most of the vertical circulations in this region are wind-driven, and a poor simulation of the Southern Ocean for the present climate can be expected to distort aspects of the large-scale response to increased anthropogenic forcing. Rates of water mass formation, and the availability of nutrients from upwelled waters, are sensitive to both atmospheric and ocean forcing, so changing the temperature or circulation patterns of either will lead to substantial changes in the sea ice and ocean productivity upon which Southern Ocean cetaceans depend.

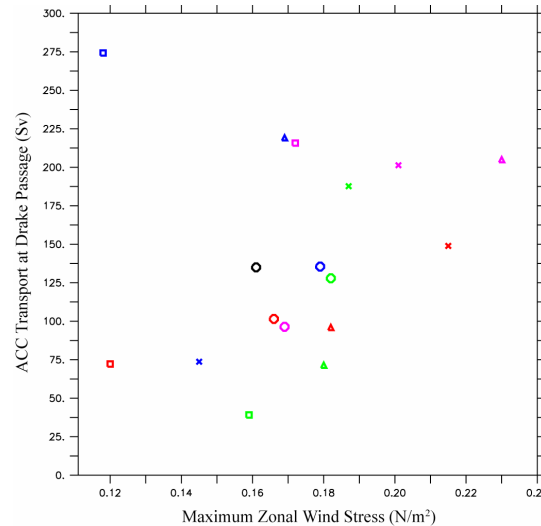
The Southern Ocean circulation is dominated by the Antarctic Circumpolar Current (ACC), the largest current in the world ocean. Due to the strength of westerly winds over the Southern Ocean, the Ekman drift in the

surface layer is substantial. This northward drift of surface waters creates a divergence south of the Polar Front, which in turn creates vast areas of upwelled water (Peterson & Whitworth, 1989). This upwelled water has a large effect on the high latitude heat flux between the atmosphere and ocean. In addition to this heat effect, the amount of relatively fresh mode and intermediate waters exported north of the ACC in the shallow overturning circulation, the density gradient across the ACC, and the relative amount of salty deep water pulled near the surface from below the sill depth of the Drake Passage south of the ACC, all affect a model's Southern Ocean and therefore will influence its response to anthropogenic forcing.

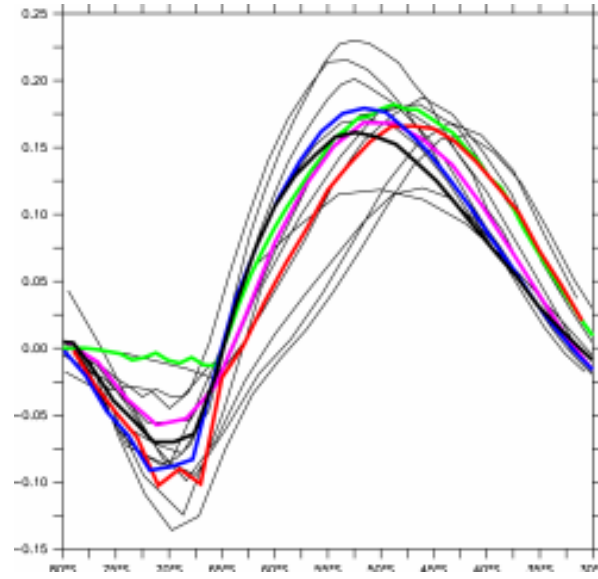
Studies using the IPCC AR4 coupled climate models (CCM) generally create what is known as an *ensemble*: an individual variable from each of the various models is averaged to derive a robust consensus from the simulations. We will show that for sea ice, model errors tend to cancel, making the ensemble used in the IPCC analysis appear better than any of the individual components. Using a set of observational criteria, the pre-industrial control and 20<sup>th</sup> century runs, we will winnow the available models on the basis of their Southern Hemisphere westerly winds and Antarctic circumpolar currents. We then narrow them further by comparing their results for sea ice and ocean frontal structure from the 20<sup>th</sup> century to the available observational record (from shipboard measurements and satellites). Next, we determine the year in which each model's globally-averaged annual-mean temperature has risen by 2°C, and use this benchmark to explore projections of how the physical environment will have changed.

### The Pre-industrial and Modern Simulations

Russell et al. (2006) evaluated 18 of the coupled climate models by comparing the relationship between the Pre-industrial westerly winds and the strength of the ACC, and we use this as our starting point. We compare the wind stress and ACC strength for the last 20 years of the 20<sup>th</sup> century run for each model (Figure 1). Several of the models are clustered close to the observations: these include the Geophysical Fluid Dynamics Laboratory (GFDL, USA) GFDL-CM2.1, GFDL-CM2.0, the Model for Interdisciplinary Research on Climate (MIROC, Japan) MIROC3.2 (high-resolution ocean simulation 'hires'), Meteorological Research Institute – Coupled General Circulation Model (MRI-CGCM, Japan) MRI-CGCM2.3.2a, Institute of Atmospheric Science, Chinese Academy of Science (IAP) IAP-FGOALS1.0g, Institute for Numerical Mathematics (INM, Russia) INM-CM3.0, and Canadian Centre for Climate Modeling and Analysis (CCCMA) CCCMA3.1-T47 simulations. As a first cut, these models seem to be producing a Southern Ocean that is reasonable: the winds and ACC circulation are relatively close to the observations.

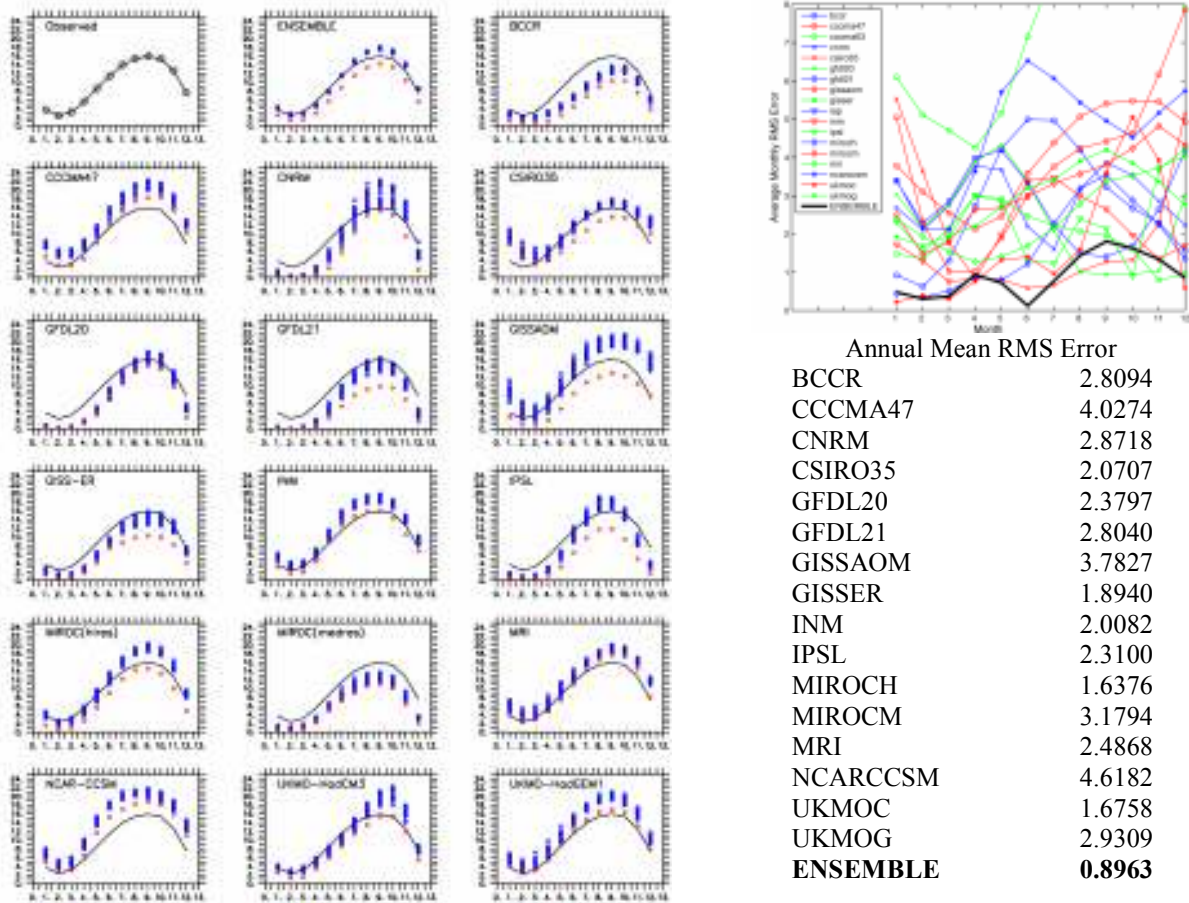


**Figure 1:** The observed long-term maximum zonally-averaged annual-mean wind stress between 70°S and 30°S ( $\text{N m}^{-2}$ ) (National Centers for Environmental Prediction) plotted against the ACC transport at Drake Passage (69°W). Observed (black circle), GFDL-CM2.1 (blue circle), GFDL-CM2.0 (red circle), CCCMA3.1-T47 (red triangle), CNRM-CM3 (red square), CSIRO-Mk3.5 (red cross), GISS-AOM (blue triangle), GISS-ER (blue square), IAP-FGOALS1.0g (blue cross), INM-CM3.0 (green triangle), IPSL-CM4 (green square), MIROC3.2 (high-resolution, 'hires') (green circle), MIROC3.2 (medium-resolution, 'medres') (green cross), MRI-CGCM2.3.2a (purple circle), NCAR-CCSM-3.0 (purple triangle), UKMO-HadCM3 (purple square), and UKMO-HadGEM1 (purple cross).



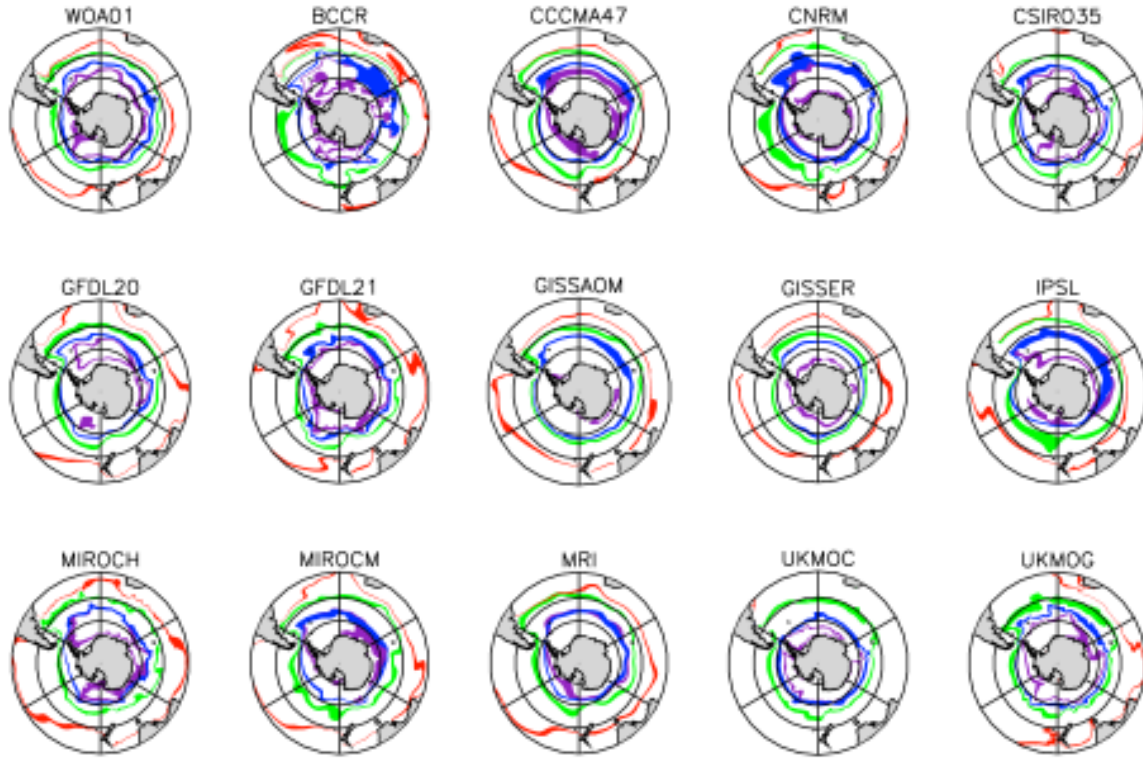
**Figure 2:** Zonally-averaged annual mean wind stress ( $\text{N m}^{-2}$ ) for the 20<sup>th</sup> century. Observed long-term mean from the National Centers for Environmental Prediction (NCEP) (thick black), GFDL-CM2.1 (blue), GFDL-CM2.0 (red), MIROC3.2 (hires) (green), and MRI-CGCM2.3.2a (purple). Models included in the original analysis but omitted from our ENSEMBLE are indicated with thin black lines and include: CCCMA3.1-T47, CNRM-CM3, CSIRO-Mk3.5, GISS-AOM, GISS-ER, INM-CM3.0, IPSL-CM4, MIROC3.2 (medres), UKMO-HadCM3, and UKMO-HadGEM1. The 20<sup>th</sup> century annual mean for the model runs is defined as the average of all months between January 1981 and December 2000.

Figure 2 shows the zonally-averaged annual-mean wind stress for the models for the last 20 years of the 20<sup>th</sup> century runs. Russell et al. (2006) noted that most of the models have a maximum wind stress equatorward of the observations, some by more than  $10^\circ$  latitude. The models chosen and highlighted in Figure 1 all have a relatively accurate wind profile; neither too weak nor too strong and a maximum within  $6^\circ$  latitude of the observed. [As we eventually eliminate the CCCMA47, IAP, and INM models from our ENSEMBLE, their wind stress curves are not separated out from the rest of the pack.]



**Figure 3:** a) The total Antarctic sea-ice area ( $10^6 \text{ km}^2$ ) for each month of the first 20 simulated years of the pre-industrial control (blue), each month of the year of  $2^\circ\text{C}$  warming (red), and from the modern observations from NCEP (black, Reynolds et al., 2002); b) the mean RMS error for each month for the total area of Antarctic sea ice for the 20 years of the pre-industrial control experiment, relative to the modern observations. The thick black line in (b) is the RMS error of the 16-member ensemble. The table indicates the annual mean of the monthly RMS error for each model.

As the next part of our winnowing process, we examined the seasonal cycle of sea ice around Antarctica (Figure 3a). Most of the models have a reasonable seasonal range of total ice area, between 0 and 20 million  $\text{km}^2$ . The modern observations still have sea ice around Antarctica in February (month of the yearly minimum), but some of the models have no sea ice at all for one or more months of the year. We chose to use a root-mean-squared error calculation so problems with too little ice in the austral summer would not be weighted as strongly as a significant error in winter. One of the models, IAP, which has nearly perpetual ice cover out to almost  $40^\circ\text{S}$ , was excluded from further consideration. Figure 3b is a clear example of why care must be taken when looking at ensembles of different models. The RMS error in June for the collection of models is significantly lower than that for any individual model.



**Figure 4:** Southern Ocean fronts from modern World Ocean Atlas observations (WOA01), and each model simulation for the end of the 20<sup>th</sup> century: the red band is the Subtropical Front (salinity between 34.9 and 35.0 at 100m); the green band is the Subantarctic Front (temperature between 4°C and 5°C at 400m), the blue band is the Polar Front (temperature minimum in the upper 200 meters between 1°C and 2°C); and the purple band is the southern boundary of the ACC (sigma-0 between 27.55 and 27.65). All definitions are after Orsi et al. (1995).

We chose to further winnow the model selection by comparing their simulations of the boundaries of the ACC to the observations record. Orsi et al. (1995) defined the northern boundary of the ACC as the Subtropical Front (salinity between 34.9 and 35.0 at 100m) and defined the southern boundary of the ACC as the surface transition from Upper Circumpolar Deep Water to the denser Lower Circumpolar Deep Water (the location of the 27.6 isopycnal at 200m). The Subantarctic Front is defined as the location of potential temperatures between 4° and 5°C at 400m, and the Polar Front is defined as the location of the temperature minimum above 200m between 1° and 2°C. After considering the model simulations of the frontal structure (Figure 4), our ENSEMBLE is comprised of the GFDL-CM2.1, GFDL-CM2.0, MIROC3.2 (hires), and MRI-CGCM2.3.2a models.



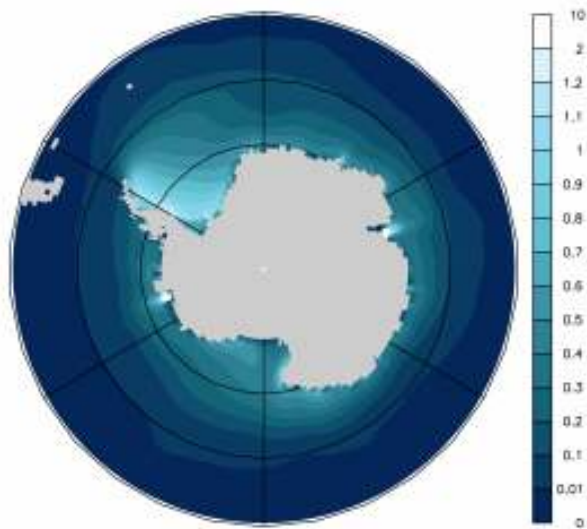


**Figure 5:** Modeled annual mean sea-ice thickness for our ENSEMBLE during the satellite era (1982-2007). Units are in meters. Darkest blue represents 0-1cm ice thickness; white represents >2m ice thickness.

As a check on the reasonableness of our choices, we now compare the simulated annual mean ice thickness from our model selection with the observational record (Timmermann et al., 2004). The models do a reasonable job of simulating the observed annual mean sea ice thickness (Figure 5). The thickest ice is in the western Weddell Sea and in the eastern Ross Sea.

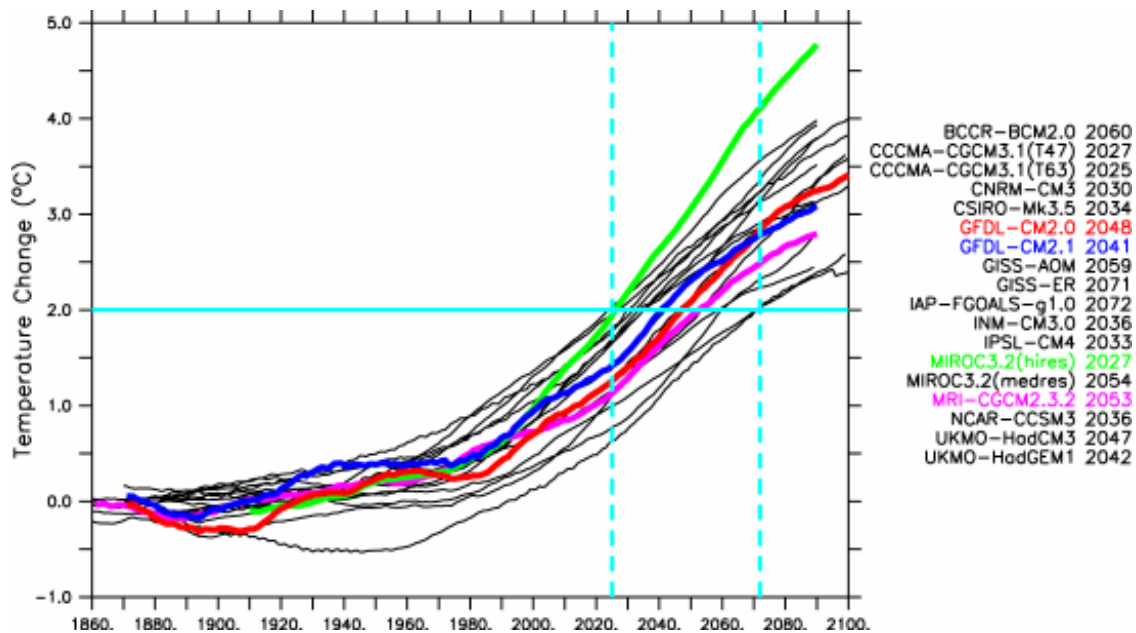


**Figure 6:** The globally-averaged annual-mean air temperature anomaly for each model. As in New (2005), a 21-year running mean filter has been applied to each time series and the year of 2°C warming is the year in which the anomaly exceeds 2°C. All runs are from the SRES A1B scenario. The colored lines are the models included in our ensemble and the black lines are the other models. The solid light blue line indicates the 2°C threshold and the dashed light blue lines bracket the times during which the models exceed this threshold.

## The Year of 2°C Warming

Rather than selecting a calendar year in the future to examine the models, we chose to compare them during their year of 2°C warming (as in New, 2005), which is defined for the purposes of this study as the year in which the globally-averaged, annual mean surface temperature has risen 2°C above the pre-industrial control simulation. This functional definition allows us to take into account differences in the sensitivities of the various models while exploring their response at a common juncture. We use the first 20 years of the control simulation after the point at which it diverged from the 20<sup>th</sup> century simulation as the baseline. That is, if the 20<sup>th</sup> century run for model X started on 1 January 1850, then we averaged the 20 years of the control run from that point onward, 1 January 1850 to 31 December 1869, in this example. The “ensemble average”, for the year in which models (Figure 7) predict an annual mean surface temperature 2°C above the pre-industrial control simulation, is 2042.

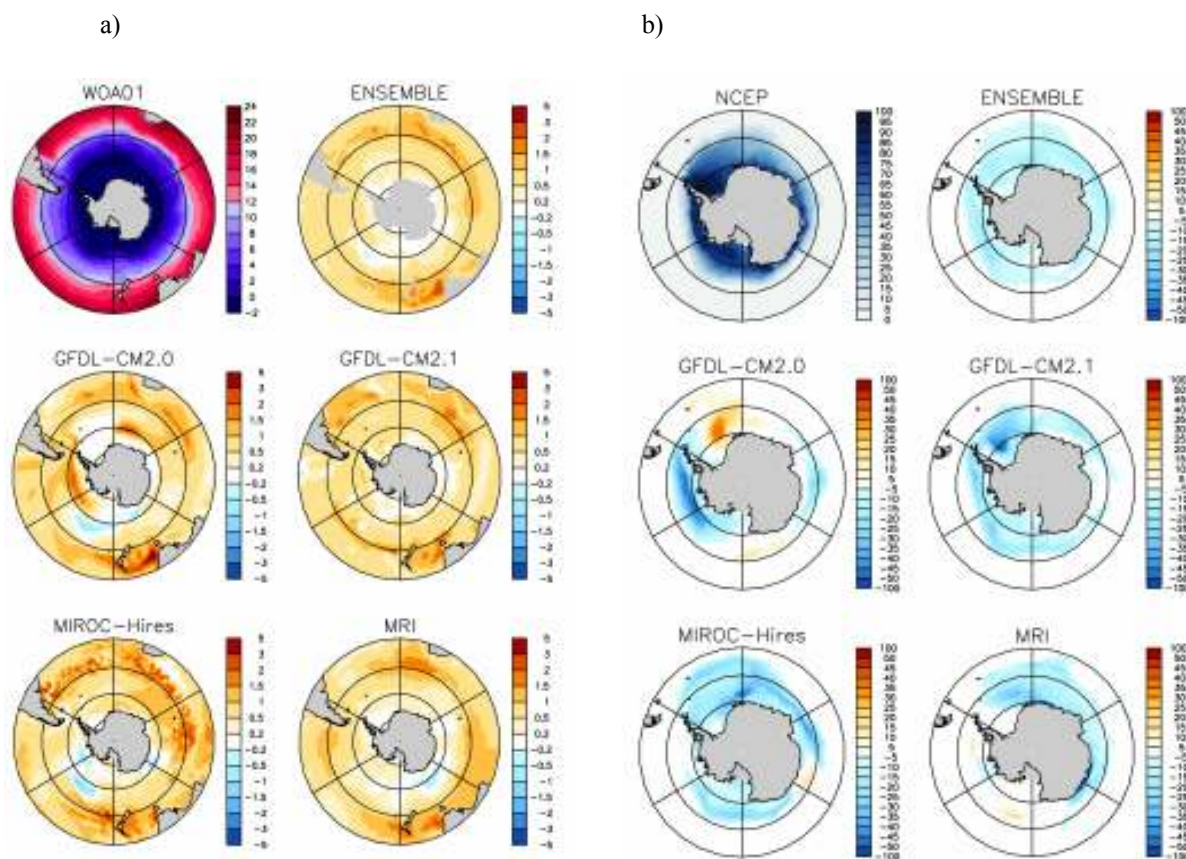


**Figure 7:** a) Observed annual mean sea surface temperatures (°C, 0-100m average) from the World Ocean Atlas (WOA01, Conkright et al., 2002) and the change in SST from the four models and the ENSEMBLE at the year of 2°C warming relative to the modern era (1981-2000 average); b) Observed annual mean sea ice coverage (%) from the National Center for Environmental Prediction reanalysis (NCEP, Reynolds et al., 2002) and the change in sea ice coverage for the four models and the ENSEMBLE at the year of 2°C warming relative to the pre-industrial control.

As expected, a warmer atmosphere leads to a warmer Southern Ocean and less sea ice around Antarctica (Figure 7). In general the ocean surface warms by more than 0.5 degrees with greater increases downstream from Australia and in the Agulhas retroflection region. These are due to changes in the circulation: a faster ACC entrains more water at its northern edge increasing the advection of warm subtropical waters in all three ocean basins. The

simulated annual mean sea ice coverage decreases by 5-10% at 60°S and by 10-15% at 70°S. The four models agree with each other with respect to changes in the sea surface temperature. There is more variability between the models with respect to projected changes in the sea ice; the GFDL-CM2.0 model shows an increase of sea ice coverage in the Weddell Sea while the GFDL-CM2.1 model indicates a decrease; the GFDL-CM2.1 modern simulation for the Southern Boundary (Figure 4) had placed this feature too far south in the Weddell Sea, and therefore may introduce far more warm UCDW than is realistic.

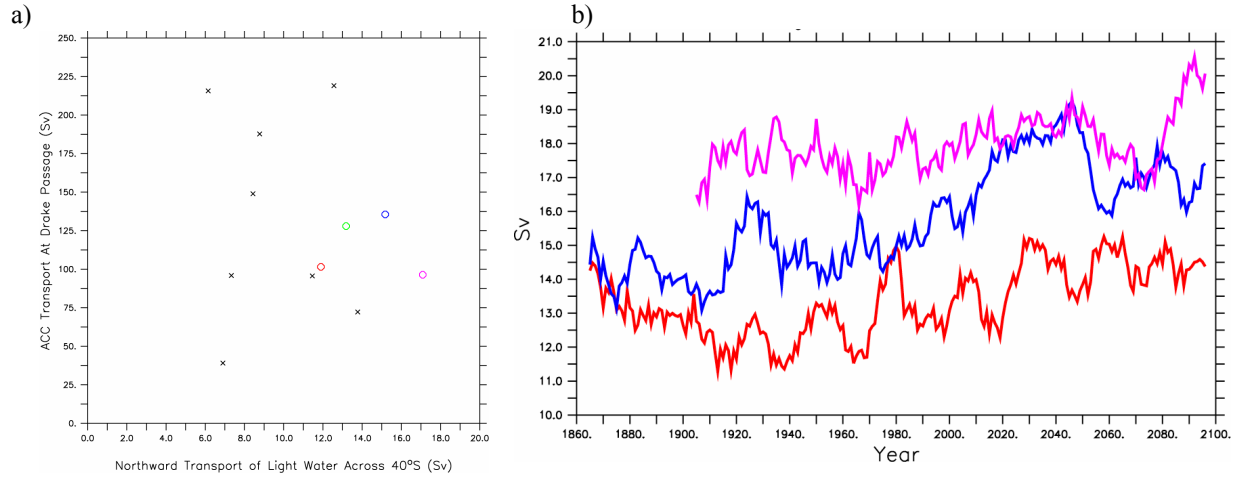


**Figure 8:** a) Northward transport of light water ( $\sigma_0 \leq 27.5$ ) at 40°S plotted against the ACC transport at Drake Passage for each of the models considered in this study. The blue circle is GFDL-CM2.1, the red circle is GFDL-CM2.0, the green circle is MIROC-3.2(hires), and the purple circle is MRI-CGCM2.3.2. The northward transport is a rough measure of the dense-to-light water transformation occurring in the Southern Ocean; b) time series of the northward transport of light water at 40°S (the conversion rate) for the GFDL-CM2.1 (blue), GFDL-CM2.0 (red) and MRI-CGCM2.3.2 (purple) coupled climate models. These time series are of the annual mean conversion rate, smoothed with a centered-mean 9-year running smoother.

The rate at which nutrients are supplied to support primary production in the Southern Ocean is influenced by the rate of upwelling. Wind forcing mechanically lifts cold water from deep in the water column (as deep as 2000m at some locations) exposes it to the surface where it can exchange heat (and carbon) with the atmosphere before it sinks again. A warmer atmosphere (as is projected by all of the coupled climate models) will impart more heat to this upwelled water. Stouffer et al. (2006) demonstrated that the main difference in the rates of atmospheric warming between the various models was due to the circulation of their Southern Ocean; as the westerly winds shift poleward, water is upwelled in greater quantities and from greater depths, sequestering more of the additional heat in the deep ocean. In the Southern Ocean, much of the water upwelled south of the Polar Front sinks back to depth, with only a small increase in temperature - not enough to transform this water into a significantly different water mass (it starts out and continues as Upper Circumpolar Deep Water). These partially equilibrated deep waters are responsible for a significant fraction of the increase in Southern Ocean heat uptake; they become even more important as the planet warms and the rest of the global ocean stratifies. One effect of this additional heat uptake can be seen in the rate at which dense water is converted into light water. Figure 8a show this conversion rate for all of the models plotted against the strength of the ACC. While there does not seem to be a significant correlation between these two factors, it is worth noting that our “better” models convert far more water than the other “lesser” models. Figure 8b shows how this conversion rate changes over time during the 20<sup>th</sup> and 21<sup>st</sup> centuries. The trend is to increased conversion and presumably increased upwelling of nutrients.



a) Southern Ocean

b) Scotia Arc

c) Kerguelen Plateau

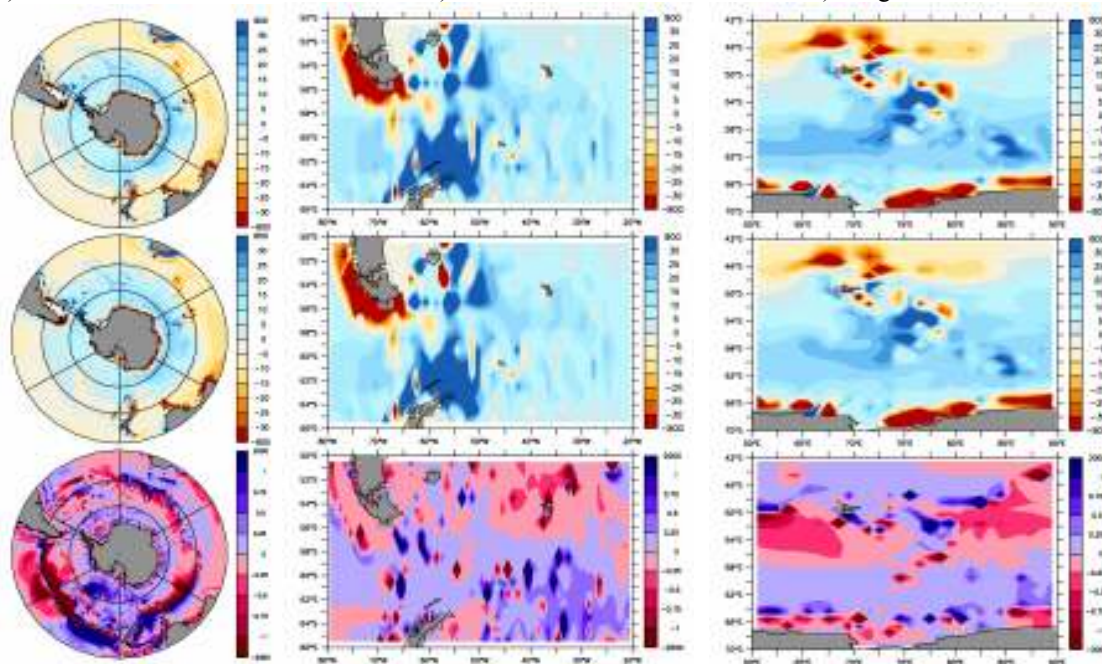


**Figure 9:** Annual mean vertical velocity of the ENSEMBLE at 200m in the year of 2°C warming (top row), and during the 20<sup>th</sup> century (middle row): blues indicate upwelling of deeper water, while reds indicate the downwelling of surface water. Units are in  $\text{cm day}^{-1}$ . The bottom row shows the fractional change in vertical velocity ( $\Delta w/w$ ) for the ENSEMBLE: blue areas indicate regions where the vertical velocity becomes more intense (both upwelling and downwelling); red areas indicate regions where the vertical motion decreases.

Most of the Southern Ocean between 70°S and 50°S has upwelling across 200m in the annual mean, both now and in the future (blue shades in the top and middle rows of Figure 9). Several regions, notably around the Scotia Arc (center column), the Kerguelen Plateau (right column) and south of the Campbell Plateau, show more intense vertical motions. The bottom row of the figure indicates regions where the vertical motion becomes more intense (either up or down) in blue as vertical mixing increases. Changes are shown relative to the modeled vertical motion, so regions with very little up or down motion can have large fractional changes (see 45°S in the Pacific Sector). Vertical motion is related to stratification and regions with decreased upwelling or downwelling are in general more stratified by the time of 2°C warming. The area downstream of the Antarctic Peninsula is, and is projected to remain, an intense upwelling area. The area around the Kerguelen Plateau, on the other hand, shows a distinct weakening of the upwelling velocity between 50°S and 55°S, along with a marginal increase in the upwelling velocity south of there.

### Circumpolar and Regions Implications of Global 2°C Warming on Cetaceans in the Southern Ocean

We now examine the circumpolar and regional patterns of change in sea surface temperature, frontal positions, and % ice cover, relative to the potential effects on cetacean populations. For comparison, two specific regions are examined in greater detail: the Scotia Arc and the area around the Kerguelen Plateau.

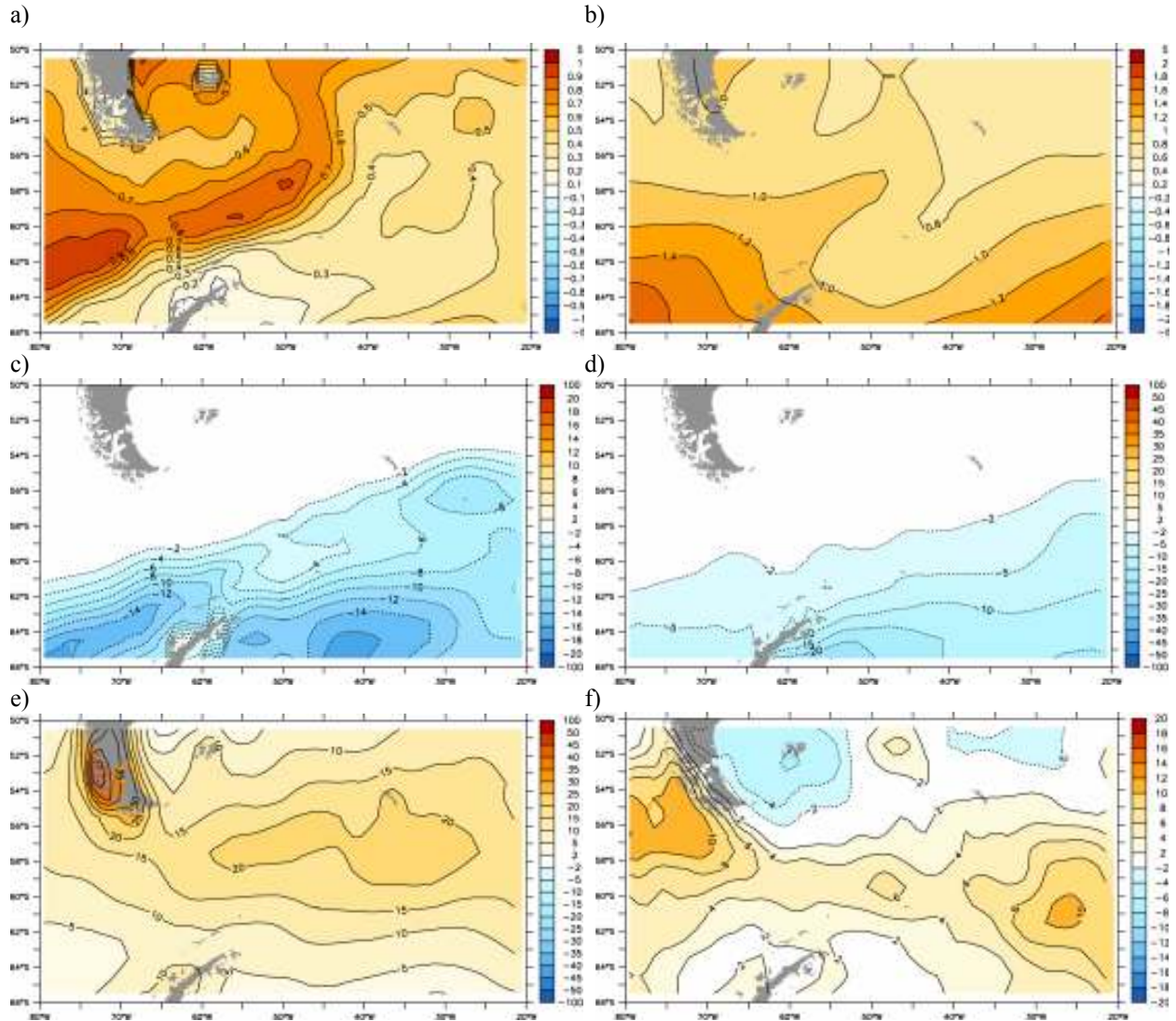


Figure 10: a) the change in annual mean sea surface temperature ( $^{\circ}\text{C}$ , 0-100m) in the Scotia Arc; b) the change in annual mean surface air temperature; c) the change in annual mean sea ice concentration (%); d) the change in the annual mean ice thickness (cm); e) the change in the annual mean zonal wind stress ( $10^{-3} \text{ N m}^{-2}$ ); and f) the change in the annual mean precipitation (cm). All panels are for the year of  $2^{\circ}\text{C}$  warming minus the mean of the last two decades of the 20<sup>th</sup> century simulation.

An examination of the changes to the physical environment in the vicinity of Scotia Arc is provided in Figure 10. The large band of surface warming is directly over the Polar Front, and the air temperature clearly responds to it. The ice edge retreats in response in the same southwest-to-northeast pattern paralleling the fronts. The increased westerly winds and slightly increased precipitation at  $60^{\circ}\text{S}$  do not have this same tilt. The rain-shadow effect of South America increases leaving the coast of southwestern Chile wetter and the Falkland Islands drier.

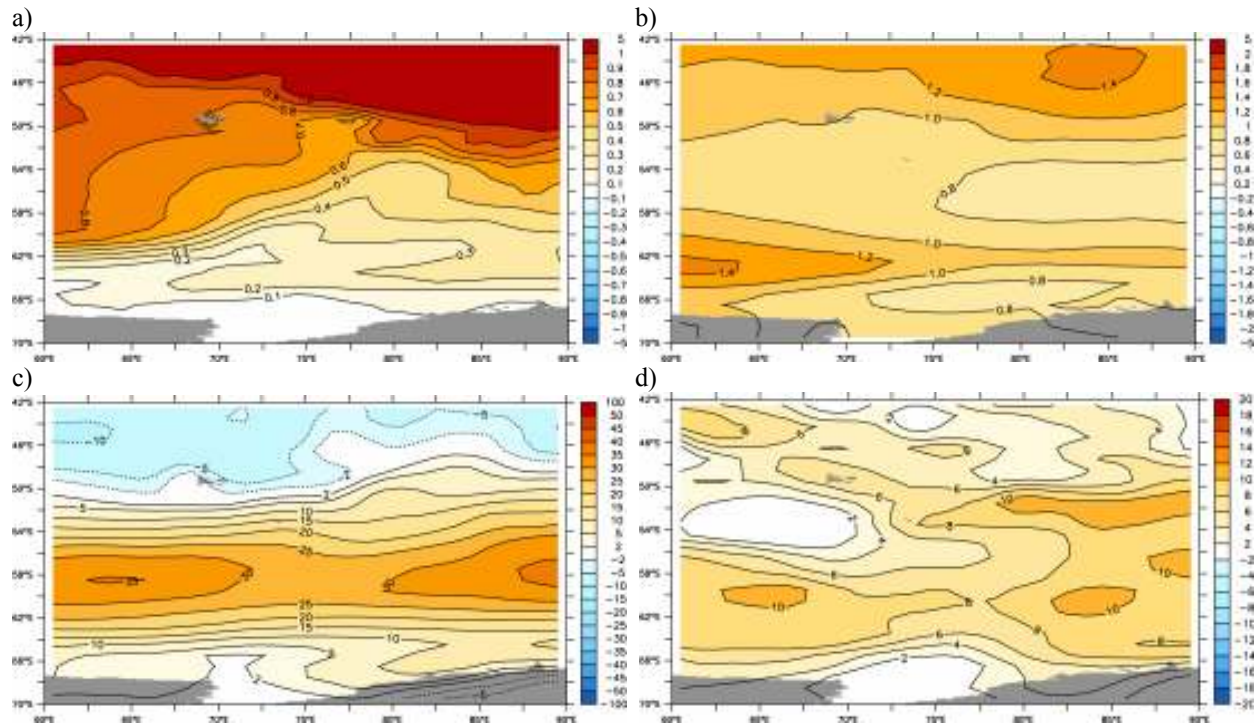


Figure 11: a) the change in annual mean sea surface temperature ( $^{\circ}\text{C}$ , 0-100m) in the Southern Indian Ocean; b) the change in annual mean surface air temperature; c) the change in the annual mean zonal wind stress ( $10^{-3} \text{ N/m}^2$ ); and d) the change in the annual mean precipitation (cm). All panels are for the year of  $2^{\circ}\text{C}$  warming minus the mean of the last two decades of the 20<sup>th</sup> century simulation.

As was noted earlier, the strong zonal wind increase (Figure 11c) drives a stronger ACC and the sea surface temperature in the southern Indian Ocean increases by over  $1^{\circ}\text{C}$  (Figure 11a) in response to the increased advection of subtropical water by the Agulhas retroflexion (Figure 11a). Otherwise changes are predominantly zonal: the surface air temperature increases by about  $1^{\circ}\text{C}$  (Figure 11b) and rainfall increases everywhere (Figure 11d).

#### *Effects of Poleward Displacement of Fronts on Cetaceans – Circumpolar*

The positions of Southern Ocean fronts, determined from IPCC models for the time of averaged global  $2^{\circ}\text{C}$  warming, vary greatly; however, the GFDL2.1 model appears to capture the most realistic late 20<sup>th</sup> c frontal patterns, especially for the Southern Boundary of the ACC, and hence provides the best prediction of frontal positions at the time of averaged global  $2^{\circ}\text{C}$  warming. At that time, the circumpolar positions of the Subantarctic Front and the Polar Front have moved southward by  $2\text{--}3^{\circ}$  latitude compared to the late 20<sup>th</sup> c position, while the position of the Southern Boundary shows less change (Figure 12). In some regions, the Polar Front and Southern Boundary of the ACC are very compressed. The potential impact of the southward displacement of the fronts is a reduction and compression of the frontal-associated habitat of Southern Ocean cetaceans around Antarctica. As these frontal features are important to migratory cetaceans (i.e., blue whale *Balaenoptera musculus*, humpback whale *Megaptera novaeangliae*, fin whale *Balaenoptera physalus*, and sperm whale *Physeter macrocephalus*; see Tynan, 1997; Tynan, 1998), it suggests a compression and reduction of valuable foraging habitat.



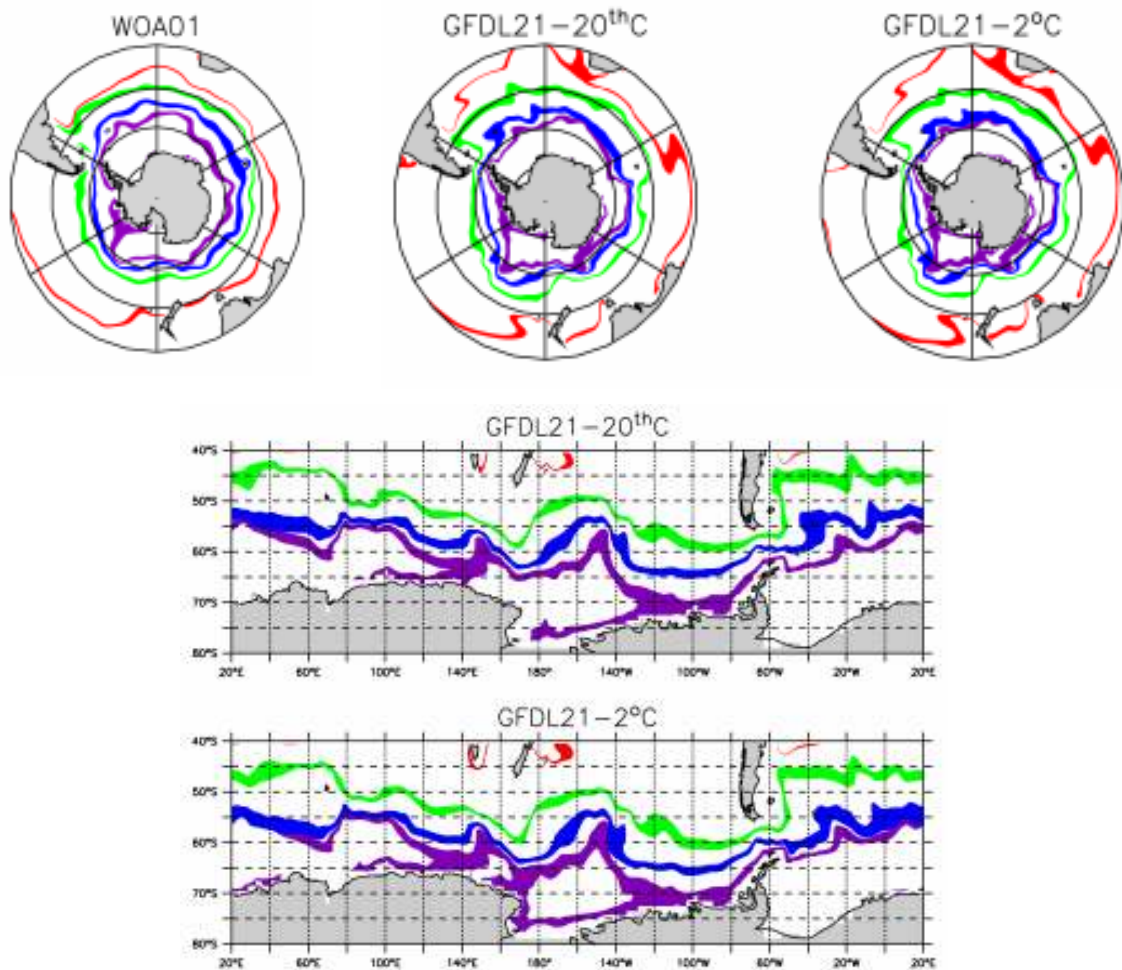


Figure 12: Southern Ocean fronts: from the modern observations (WOA01); GFDL-CM2.1 for the end of the 20<sup>th</sup> century; and GFDL-CM2.1 for the year of 2°C warming. The red band is the Subtropical Front (salinity between 34.9 and 35.0 at 100m); the green band is the Subantarctic Front (temperature between 4°C and 5°C at 400m), the blue band is the Polar Front (temperature minimum in the upper 200 meters between 1°C and 2°C); and the purple band is the southern boundary of the ACC (sigma-0 between 27.55 and 27.65). All definitions are after Orsi et al. (1995).

#### *Effects of Poleward Displacement of Fronts on Cetaceans – Regional examples*

A more detailed examination of the modeled fronts near the Scotia Arc is shown in Figure 13. At the time of averaged global 2°C warming, all fronts in Drake Passage have shifted poleward and are further displaced eastward by several °longitude in the Scotia Sea, as if the stronger ACC transport through the Drake Passage has “jetted” them further downstream. Both observations and the ENSEMBLE of selected models show the Polar Front to the west of South Georgia during the end of the 20<sup>th</sup> c. At the time of 2°C warming, the Polar Front surrounds South Georgia and the Southern Boundary of the ACC is displaced further to the east.

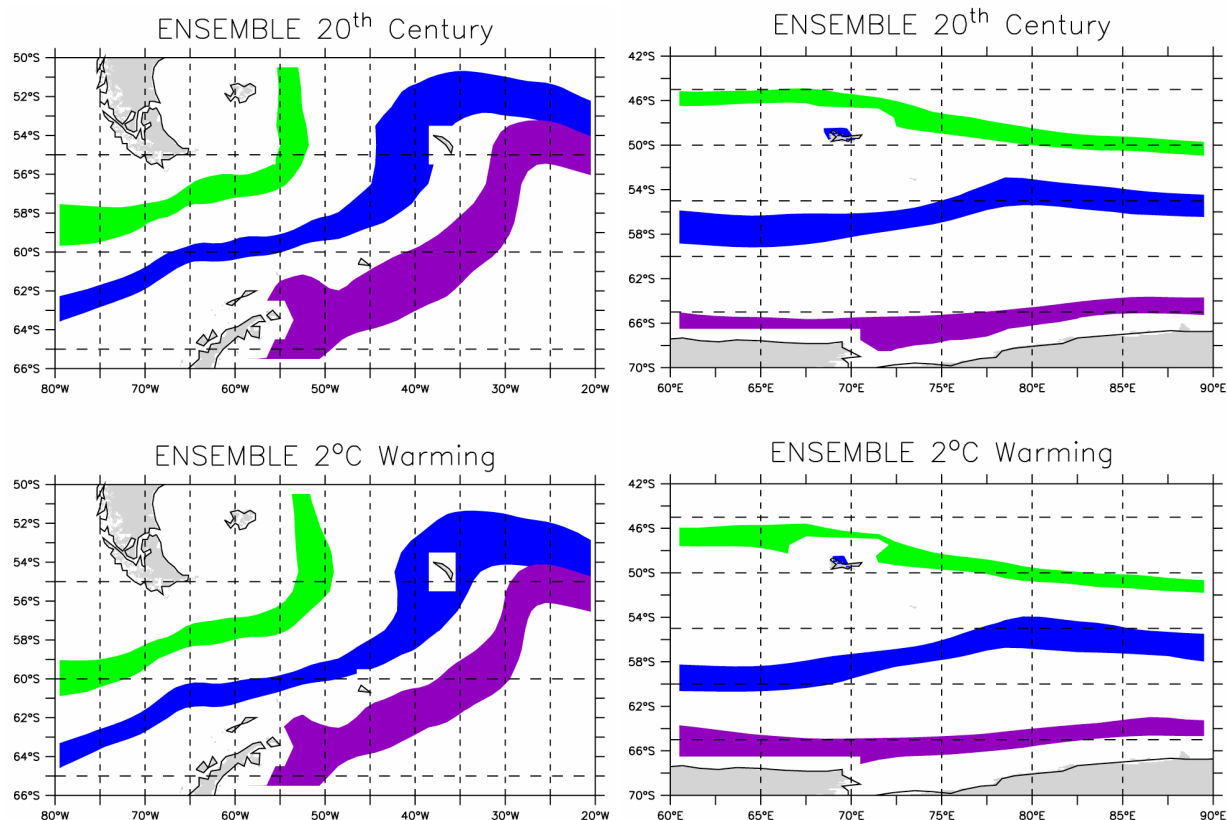


Figure 13. Modeled positions of fronts in the Drake Passage and Scotia Sea (left) and the Kerguelen Plateau region (right) shown for the ENSEMBLE for the end of the 20<sup>th</sup> century, and the ENSEMBLE for the year of 2°C warming. The green band is the Subantarctic Front (temperature between 4°C and 5°C at 400m), the blue band is the Polar Front (temperature minimum in the upper 200 meters between 1°C and 2°C); and the purple band is the Southern Boundary of the ACC (sigma-0 between 27.55 and 27.65). All definitions are after Orsi et al. (1995).

Near the Kerguelen Plateau, the Subantarctic and Polar Fronts also shift poleward by ~3° latitude (Figure 13). The Polar Front and the Southern Boundary of the ACC are closer together at the time of 2°C warming, representing a compression in the cetacean frontal habitats as well. Higher occurrences of minke whales, humpback whales, sperm whales, killer whales and southern bottlenose whales (*Hyperoodon planifrons*) are associated with the frontal features at the southern and eastern edges of the plateau, where the Southern ACC Front and Southern Boundary of the ACC follow the edge of the plateau and the Princess Elizabeth Trough (Tynan, 1996; Tynan 1997). These are among the species that would be affected by the poleward compression of fronts. The coupled climate models do not provide sufficient resolution of eddy-activity south and east of the plateau, which has also been shown to be important to cetaceans in this region (Tynan, 1997).

#### *Effects of loss of sea-ice coverage – Circumpolar*

The change in % sea-ice coverage determined from the four models, and the combined ENSEMBLE, at the year of 2°C warming, relative to the pre-industrial control, shows a loss of the regional % sea-ice coverage from 5-30%, with greatest ice loss in the Weddell Sea and western Antarctic Peninsula regions (Figure 7, Figure 14). Since 1980, the Antarctic Peninsula region has experienced the largest positive temperature anomalies of the Southern Hemisphere (Overland et al., 2008) and our selection of climate models predict that this region will continue to experience among the greatest loss of sea ice.

For the ice-associated Antarctic minke whale *Balaenoptera bonaerensis*, a denizen of the pack-ice habitat (Aguayo-Lobo, 1994; Ainley et al. 2007), the loss of sea-ice would likely also result in a reduction of available ice-associated prey (i.e. krill *Euphausia superba*). Depending on the Antarctic sector, Antarctic minke whales are predicted to lose



5-30% of ice-associated habitat by the time of 2°C globally-averaged warming, along with a reduction of ice-associated prey. The life-cycle of krill has evolved in association with sea-ice and regional circulation patterns (see Nicol et al., in press). Larval krill have an overwintering strategy that includes feeding on ice algae scraped from the underside of annual ice (Daly, 1990). Thus, krill occur in regions that are covered by ice in winter, and their life cycle is closely related to the oscillation of sea ice cover (Brierley and Thomas, 2002). Krill also graze on ice algae at the ice edge in the marginal ice zone (Daly and Macaulay, 1991). All these linkages between krill and sea ice suggest that a reduction in ice-habitat would co-occur with a reduction in krill production.

It is estimated that an increase in open water of 25% in the Southern Ocean may enhance primary production by 10% (Arrigo and Thomas, 2004); however, it has been observed in many parts of the global coastal ocean that increases in primary production and increased blooms, associated with warming trends, are often accompanied by ecologically undesirable or harmful shifts in the phytoplankton species assemblage (Kahru and Mitchell, 2008). For example, there is some evidence that warming along the Antarctic Peninsula has contributed to a shift in the phytoplankton community from large diatoms, which krill prefer to eat, to small cryptophytes (Moline et al., 2004). Another cause for concern in neritic regions are shifts during summer from ice-associated blooms of diatoms to the presence of the gelatinous colonial prymnesiophyte *Phaeocystis antarctica*, which can form large aggregations and is considered less favorable prey for euphausiids. Krill prefer to forage on diatoms within the range of 5-40 µm, with optimal size at 25 µm foraging (Morris, 1984). Euphausiids graze *Phaeocystis* at reduced rates compared to diatoms (Hansen et al. 1994) and the ability of *E. superba* to graze on *Phaeocystis* decreases with increasing colony size (Haberman et al. 2003). Further, the projected intensification and poleward shift in Westerly winds could enhance mixing, producing conditions which favor *Phaeocystis* blooms (Arrigo et al. 1999) rather than the diatom blooms that occur with well-stratified conditions near the ice edge. Therefore, it is possible that krill populations will be diminished as both a direct loss of ice habitat and shifts in the preferred phytoplankton prey.

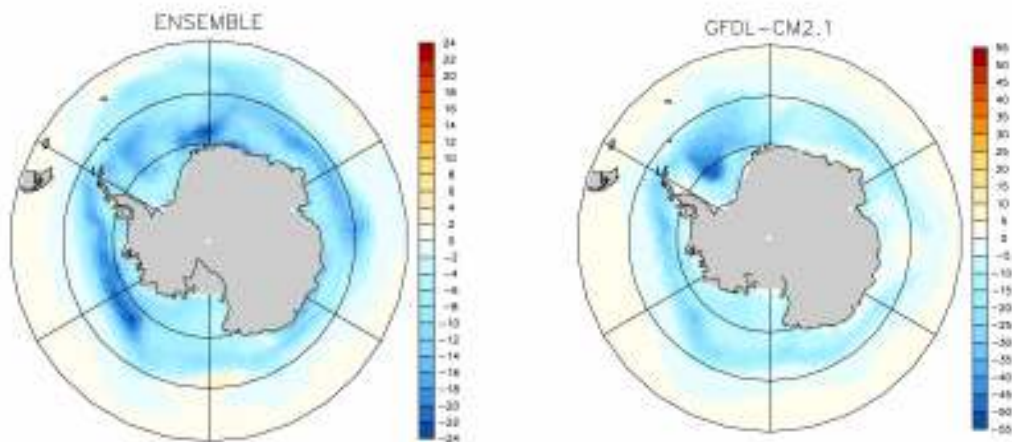


Figure 14. Change in % sea-ice coverage for the ENSEMBLE of models, and the GFDL-CM2.1 model, at the year of 2°C warming relative to the pre-industrial control.

#### *Effects of loss of sea-ice coverage – Regional*

At the time of globally-averaged 2°C warming, the greatest loss of sea-ice coverage, 20-30% loss, is expected to occur in: the Pacific Sector and West Antarctic Peninsula; Scotia Arc, Weddell Sea and Atlantic Sector (Figure 14). The ENSEMBLE predicts that the southern Indian Ocean sector will have lost 10-20% of ice cover. The loss of ice would be expected to affect resident Antarctic minke whales and migratory cetacean populations most strongly in these regions. Ainley et al. (2007) found a higher probability of Antarctic minke whale presence farther into the pack ice in the Amundsen and southern Bellingshausen Sea Sector. The lack of such baseline survey effort in pack ice during circumpolar IDCR-SOWER cruises raises questions about whether Antarctic minke whale assessments are suitable to gauge climate-related movements of minke whales or population trends related to observed and predicted loss of ice habitat. Branch (2007) found a decline in Antarctic minke whale abundance during the third circumpolar set of IDCR-SOWER cruises (1991/92-2003/4); estimates were low and only 18-52% of CPII estimates for Areas I-V. Unanswered questions remain, as to whether the decline reflects movement patterns into the ice, or whether the population has declined. Given model predictions that by ~ 2042 ice-associated habitat for Antarctic

minke whales will have declined by 20-30% in some sectors (Figure 14), and likely that their prey availability will decline as well, projections of population change should not be based on IDCR-SOWER surveys which lack baseline pack-ice survey effort during the late 20<sup>th</sup> century. The loss of ice habitat for Antarctic minke whales could result in apparent increased densities of whales in suitable pack ice nearer the continent, as ice cover shrinks, and in lower populations as a result of reduced prey abundance.

In the Southeast Pacific Sector, the shrinkage of the marginal ice zone would also result in a loss of summer and fall ice-edge habitat for migratory and resident cetacean populations. Along the West Antarctic Peninsula (WAP), the shelf distribution of humpback and minke whales is tightly coupled to the distribution and abundance of their prey, and to the sea-ice boundary (Thiele et al., 2004; Friedlaender et al., 2006). The WAP is among the regions predicted to experience the greatest loss of sea ice (Figure 12), and consequently, a loss of important foraging habitat for humpback and minke whales.

In the South Atlantic Sector, Scotia Arc, the loss of sea-ice coverage could affect the movements and foraging of minke whales and blue whales, which appear to migrate through open waters to the ice-edge zone to feed (Reilly et al., 2004). The ENSEMBLE of models predicts that whales in the South Atlantic Sector, approaching the Weddell Sea, would encounter a 10-20 % reduction in ice coverage at the time of 2°C warming (Figure 12); the GFDL-CM2.1 model shows a greater reduction of ice coverage of 10-40%.

## SUMMARY

Coupled climate models submitted for the 4<sup>th</sup> Assessment of the IPCC were analyzed and evaluated for their representation of the Southern Ocean and their predictions for change in ice cover and fronts that will impact cetaceans. The “best” four models were composited into an ensemble which was then examined at the year of 2°C warming. Varying with specific Southern Ocean sector, Antarctic minke whales *Balaenoptera bonaerensis* are expected to lose 5-30% of ice-associated habitat in the Antarctic by the year of 2°C warming (i.e., 2042 for the ensemble average). Migratory cetaceans will travel farther (~3-5° latitude) to reach important Southern Ocean fronts where they forage. The potential impact of the southward displacement of Southern Ocean fronts and watermass boundaries (i.e. Polar Front and Southern Boundary of the ACC) is a reduction and compression of the frontal-associated habitat of Southern Ocean cetaceans around Antarctica. As these frontal features are seasonally important to migratory cetaceans (i.e., blue whale *Balaenoptera musculus*, humpback whale *Megaptera novaeangliae*, fin whale *Balaenoptera physalus*, and sperm whale *Physeter macrocephalus*), it suggests a compression and reduction of valuable foraging habitat. By the time of 2°C warming, the loss of 5-30% of ice cover is expected to reduce the availability of krill *Euphausia superba* upon which resident and migratory cetaceans, and the Antarctic ecosystem, depends.

## References

- Aguayo Lobo, A. 1994. Is there a population of minke whales that overwinter among the Antarctic sea-ice? *Ser. Cient. Inst. Antart. Chil.* 44: 91-98.
- Ainley, D.G., Dugger, K.M., Toniolo, V. and Gaffney, I. 2007. Cetacean occurrence patterns in the Amundsen and southern Bellingshausen Sea sector, Southern Ocean. *Mar. Mamm. Sci.* 23: 287-305.
- Arrigo, K.R. and Thomas, D.N. 2004. Large scale importance of sea ice biology in the Southern Ocean. *Antarctic Science* 16(4): 471-486.
- Arrigo, K.R., Worthen, D., Schnell, A., Lizotte, M.P. 1998. Primary production in Southern Ocean waters. *Journal of Geophysical Research* 103(C8): 15,587-15,600.

- Arrigo, K.R., Robinson, D.H., Worthen, D.L., Dunbar, R.B., DiTullio, G.R., VanWoert, M. and Lizotte, M.P. 1999. Phytoplankton community structure and the drawdown of nutrients and CO<sub>2</sub> in the southern ocean. *Science* 283: 365-367.
- Branch, T.A. 2007. Abundance estimates for Antarctic minke whales from three completed circumpolar sets of surveys, 1978/79 to 2003/04. IWC SC/58/IA18.
- Brierley, A.S. and Thomas, D.N. 2002. On the ecology of the Southern Ocean pack ice. *Advances in Marine Biology* 43: 171-278.
- Conkright, M.E., Locarnini, R.A., Garcia, H.E., O'Brien, T.D., Boyer, T.P., Stephens, C. and Antonov, J.I. 2002. World Ocean Atlas 2001: Objective Analyses, Data Statistics, and Figures, CD-ROM Documentation. National Oceanographic Data Center, Silver Spring, MD, 17 pp.
- Daly, K.L. 1990. Overwintering development, growth and feeding of larval *Euphausia superba* in the Antarctic marginal ice zone. *Limnology and Oceanography* 35: 1564-1576.
- Daly, K.L. and Macaulay, M.C. 1991. Influence of physical and biological mesoscale dynamics on the seasonal distribution and behavior of *Euphausia superba* in the Antarctic marginal ice zone. *Mar. Ecol. Prog. Ser.* 79: 37-66.
- Friedlaender, A.S., Halpin, P.N., Qian, S.S., Lawson, G.L., Wiebe, P.H., Thiele, D. and Read, A.J. 2006. Whale distribution in relation to prey abundance and oceanographic processes in shelf waters of the Western Antarctic Peninsula. *Mar. Ecol. Prog. Ser.* 317: 297-310.
- Haberman, K.L., Quentin, L.B. and Ross, R.M. 2003. Diet of the Antarctic krill (*Euphausia superba* Dana) – I. Comparisons of grazing on *Phaeocystis antarctica* (Karsten) and *Thalassiosira antarctica* (Comber). *J. Exp. Mar. Biol. Ecol.* 283: 79-95.
- Hansen, B., Verity, P., Falkenhaus, T., Tande, K.S., and Norrbin, F. 1994. On the trophic fate of *Phaeocystis pouchetti* (Harriot). V. Trophic relationships between *Phaeocystis* and zooplankton: an assessment of methods and size dependence. *J. Plankton Res.* 16: 487-511.
- IPCC, 2007: Climate Change 2007: The Physical Science Basis. Contribution of Working Group I to the Fourth Assessment Report of the Intergovernmental Panel on Climate Change [Solomon, S., D. Qin, M. Manning, Z. Chen, M. Marquis, K.B. Averyt, M. Tignor and H.L. Miller (eds.)]. Cambridge University Press, Cambridge, United Kingdom and New York, NY, USA, 996 pp.
- Kalnay et al. 1996. The NCEP/NCAR 40-year reanalysis project. *Bull. Amer. Meteor. Soc.* 77: 437-470.
- Kahru, M and Mitchell, B.G. 2008. Ocean color reveals increased blooms in various parts of the world. *EOS* 89:170.
- Moline, M.A., Claustre, H., Frazer, T., Schofield, O. and Vernet M. 2004. Alteration of the foodweb along the Antarctic Peninsula in response to a regional warming trend. *Global Change Biology* 10: 1973-1980.
- Morris, D.J. 1984. Filtration rates of *Euphausia superba* Dana: under- or overestimates? *J. Crustacean Biol.* 4: 185-197.
- New, M.G. 2005. Arctic climate change with a 2°C global warming. In: Rosentrater LD (ed) Evidence and implications of dangerous climate change in the Arctic. WWF, Oslo, 1-15.
- Nicol, S., Worby, A. and Leaper, R. 2008. Changes in the Antarctic sea ice ecosystem: potential effects on krill and baleen whales. *Marine and Freshwater Research* (in press).
- Orsi, A.H., Whitworth, T.W. III, and Nowlin, W.D. Jr. 1995. On the meridional extent and fronts of the Antarctic Circumpolar Current. *Deep-Sea Res., Part I*, 42: 541-673.

- Overland, J., Turner, J., Francis, J., Gillett, N., Marshall, G., and Tjernström, M. 2008. The Arctic and Antarctic: Two faces of climate change. *EOS* 89(19): 177-178.
- Peterson, R.G. and Whitworth III, T. 1989. The subantarctic and polar fronts in relation to deep water masses through the southwestern Atlantic. *J. Geophys. Res.* 94: 10,817-10,838.
- Reilly, S., Hedley, S., Borberg, J., Hewett, R., Thiele, D., Watkins, J. and Naganobu, M. 2004. Biomass and energy transfer to baleen whales in the South Atlantic Sector of the Southern Ocean. *Deep-Sea Res. II* 51: 1397-1409.
- Reynolds, R.W., Rayner, N.A., Smith, T.M., Stokes, D.C. and Wang, W. 2002. An improved in situ and satellite SST analysis for climate. *J. Climate* 15: 1609-1625.
- Russell, J.L., Stouffer, R.J., and Dixon, K.W. 2006. Intercomparison of the Southern Ocean circulations in IPCC Coupled Model Control simulations. *J. Climate* 19: 4560-4575.
- Stouffer, R.J., Russell, J.L. and Spelman, M.J. 2006. Importance of Oceanic Heat Uptake in Transient Climate Change. *Geophys. Res. Lett.* 33, L17704, doi:10.1029/2006GL027242.
- Thiele, D.C., Chester, E.T., Moore, S.E., Sirovic, A., Hildebrand, J.A., and Friedlaender, A.S. 2004. Seasonal variability in whale encounters in the West Antarctic Peninsula. *Deep-Sea Res. II* 51: 2311-2325.
- Timmermann, R., Worby, A., Goosse, H. and Fichefet, T. 2004. Utilizing the ASPeCt sea ice thickness data set to evaluate a global coupled sea ice-ocean model. *J. Geophys. Res.* 109, C07017, doi:10.1029/2003JC002242.
- Tynan, C.T. 1996. Characterization of oceanographic habitat of cetaceans in the Southern Indian Ocean between 82° – 115° E: Cruise report from the World Ocean Circulation Experiment (WOCE) I8S and I9S. U.S. Dep. Commer., NOAA Tech. Memo. NMFS-AFSC-64, 53 p.
- Tynan, C.T. 1997. Cetacean distributions and oceanographic features near the Kerguelen Plateau. *Geophys. Res. Lett.* 24: 2793-2796.
- Tynan, C.T. 1998. Ecological importance of the southern boundary of the Antarctic Circumpolar Current. *Nature* 392: 708-710.